Materials and Design 32 (2011) 3347–3353

Contents lists available at ScienceDirect

Materials and Design

journal homepage: www.elsevier.com/locate/matdes

# Effects of sintering parameters on the microstructure and tensile properties of *in situ* TiBw/Ti6Al4V composites with a novel network architecture

L.J. Huang [a], L. Geng [a,*], H.X. Peng [b], K. Balasubramaniam [a], G.S. Wang [a]

[a] School of Materials Science and Engineering, Harbin Institute of Technology, P.O. Box 433, Harbin 150001, China
[b] Advanced Composites Centre for Innovation and Science (ACCIS), Bristol University, Bristol, BS8 1TR, United Kingdom

ARTICLE INFO

*Article history:*
Received 26 November 2010
Accepted 5 February 2011
Available online 12 February 2011

*Keywords:*
A. Metal matrix composites
C. Powder metallurgy
F. Microstructure

ABSTRACT

In order to better understand the relationship of processing–structure–mechanical properties of *in situ* TiB whisker reinforced Ti6Al4V (TiBw/Ti64) composites with a novel network architecture, the effects of sintering parameters on the microstructure and tensile properties of the composites were investigated. TiB whiskers with the highest aspect ratio and the coarsest whiskers were obtained at 1100 °C and 1200 °C due to the skips of whisker growth speeds along the [0 1 0] direction and the [0 0 1] and [1 0 0] directions, respectively. Additionally, TiB whisker with a claw-like structure can be synthesized from one $TiB_2$ polycrystal parent. The quasi-continuous network architecture of TiBw/Ti64 composites can be achieved at higher sintering temperatures more than 1200 °C. The prepared composites with the quasi-continuous network architecture exhibit a superior combination of tensile properties.



## 1. Introduction

Titanium matrix composites (TMCs) attract much more attention due to their high special strength, high special stiffness, excellent wear resistance and high temperature durability, which render them as the optimal candidate material for a range of commercial automotive, aerospace and military applications [1,2]. TMCs can be divided into the continuous fiber reinforced titanium matrix composites (CRTMCs) [3] and the discontinuous particle and/or whisker reinforced titanium matrix composites (DRTMCs) [4,5]. Furthermore, the discontinuous TiB whiskers and/or TiC particles [1,2,6] reinforced titanium matrix composites fabricated by *in situ* methods are sought-after due to their superior and isotropic properties and low cost. Moreover, TiB whiskers are regarded as the optimal reinforcement not only because of its high modulus and hardness and good chemical compatibility with Ti matrix but also its similar density and thermal expansion coefficient with Ti matrix [2,7]. Powder metallurgy (PM) process, one of *in situ* methods, has been considered to be an excellent method to fabricate TMCs largely due to its ability for microstructural control, near net shape processing, minimal material waste and low cost [8].

Irrespective of the method and reinforcement used, the aim is always to obtain a homogeneous reinforcement distribution where the reinforcements are uniformly dispersed in titanium matrix [2,7,9]. However, many TMCs with the homogeneous microstructure exhibit a limited improvement of mechanical properties, even inferior mechanical properties such as extreme brittleness for TMCs fabricated by the conventional PM processes including high energy milling, isostatic cool pressing, sintering and extrusion [2,7,8].

Fortunately, it was well demonstrated that the serious drawbacks have been solved by tailoring a novel network reinforcement distribution of TiBw/Ti64 composites fabricated by a simplified PM process in our previous work [1]. Not only TMCs with the network microstructure exhibited a superior combination of properties, but also the fabrication processes were significantly simplified by using the low-energy milling and one-step sintering processes without any subsequent treatment such as extrusion. On the one hand, different raw materials require different sintering parameters, and on the other hand, the formation mechanism of branched and dowel-like TiBw structures which can exploit a better strengthening effect has not been reported up to now. Therefore, it is certainly interesting and important to investigate the effects of sintering parameters on the microstructure (the nucleation and growth of TiB whisker) and tensile properties of *in situ* TiBw/Ti64 composites with a novel network microstructure.

## 2. Experimental procedure

The spherical Ti64 powders with a large size of 180–220 μm (Fig. 1a), prismatic $TiB_2$ powders with a small size of 1–8 μm (Fig. 1b) were selected in the present study in order to obtain the network reinforcement architecture. The chemical composition of

* Corresponding author. Tel.: +86 451 86418836; fax: +86 451 86413922.
*E-mail addresses:* ljhuanghit@yahoo.com.cn (L.J. Huang), genglingroup@gmail.com, genglin@hit.edu.cn (L. Geng).

0261-3069/$ - see front matter © 2011 Elsevier Ltd. All rights reserved.
doi:10.1016/j.matdes.2011.02.023

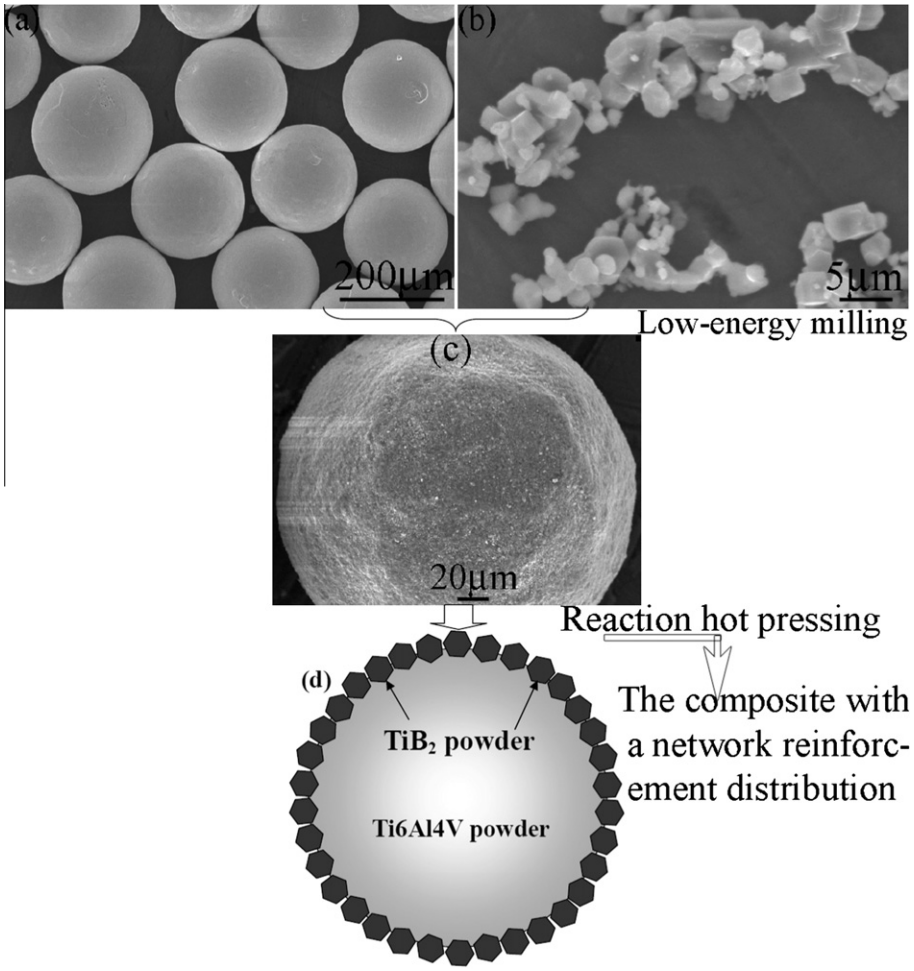


**Fig. 1.** Flow chart of fabrication of TiBw/Ti64 composites with a network microstructure and SEM micrographs of raw materials and the mixture: (a) Ti64 powder (180–220 μm), (b) $TiB_2$ powder (1–8 μm), (c) the mixture of Ti64 and $TiB_2$, and (d) schematic illustration showing that $TiB_2$ powders were adhered onto the surface of Ti64 powder.

the selected Ti64 powders (in wt.%) is 6.42Al, 4.12 V, 0.16Fe, 0.12O, 0.024Si, 0.028 others, and balance titanium.

The large Ti64 and small $TiB_2$ powders were low-energy milled at a low speed of 200 rpm for a period of 8hrs. The fine $TiB_2$ powders adhered onto the surface of the large Ti64 particles by the simplified low-energy milling process as shown in Fig. 1c and d. All the milling processes were carried out under a protective argon atmosphere. To obtain the optimal fabrication parameters and further explore the effects of sintering temperature and holding time on the microstructure and mechanical properties of TMCs with a network microstructure, a range of TiBw/Ti64 composites were fabricated at 1000 °C, 1100 °C, 1200 °C and 1300 °C for a constant holding time of 1.0 h, and another two were fabricated at a constant sintering temperature of 1200 °C but for different holding times of 0.5 h and 1.5 h, respectively. Then the blended mixtures were hot pressed in vacuum ($10^{-2}$ Pa) under a pressure of 20 MPa at the different sintering temperatures (1000 °C, 1100 °C, 1200 °C and 1300 °C) and for different times (0.5 h, 1.0 h and 1.5 h) according to the above design. TiB whiskers can be synthesized according to the following reaction equation:

$$Ti + TiB_2 \rightarrow 2TiB \quad (1)$$

The nominal volume fraction of TiBw reinforcement in all the TMCs is 5 vol.%. $T_{1000}t_{1.0}$, $T_{1100}t_{1.0}$, $T_{1200}t_{1.0}$ and $T_{1300}t_{1.0}$ are represented as the 5 vol.%TiBw/Ti64 composites fabricated at 1000 °C, 1100 °C, 1200 °C and 1300 °C, respectively, for a constant holding time of 1.0 h, and $T_{1200}t_{0.5}$ and $T_{1200}t_{1.5}$ are represented as the 5 vol.%TiBw/Ti64 composites fabricated at 1200 °C but for different holding times of 0.5 and 1.5 h, respectively. These signs are also listed in Table 1. '*T*' represents the sintering temperature while '*t*' the holding time.

Tensile tests were carried out using an Instron-5569 universal testing machine at a constant crosshead speed of 0.5 mm/min. Tensile specimens have gauge dimensions of 15 mm × 5 mm × 2 mm and a total of five specimens were tested for each material. Microstructural examination was performed using a scanning electron microscope (SEM, Hitachi S-4700).

## 3. Results and discussions

### 3.1. Microstructure

Fig. 2 shows a network morphology of reinforcement distribution in the 5 vol.%TiBw/Ti64 composites fabricated at the lowest temperature (1000 °C, Fig. 2a) and the highest temperature (1300 °C, Fig. 2b), respectively. It is quite obvious that many pores which are large in size retain while fabricating the composite at the lowest temperature (1000 °C) as shown in the insert image of Fig. 2a). However, increasing the sintering temperature up to 1300 °C can totally eliminate these pores and form a compact composite as shown in Fig. 2b. On the one hand, increasing temperature softens the Ti64 matrix, and on the other hand, more adequate exothermic reactions of Ti and $TiB_2$ at the highest

**Table 1**
Tensile properties of *in situ* 5 vol.%TiBw/Ti64 composites fabricated by different sintering parameters.

| Sintering temperature (°C) | Holding time (h) | Yield strength (MPa) | Ultimate strength (MPa) | Elongation (%) | Elastic modulus (GPa) |
|---|---|---|---|---|---|
| 1000 | 1.0 | – | 318 ± 7 | – | 117.3 ± 0.5 |
| 1100 | | – | 736 ± 5 | – | 122.1 ± 0.5 |
| 1200 | | 970 ± 6 | 1112 ± 6 | 3.0 ± 0.5 | 123.1 ± 0.6 |
| 1300 | | 973 ± 5 | 1101 ± 7 | 2.8 ± 0.4 | |
| 1200 | 0.5 | 969 ± 4 | 1116 ± 5 | 2.5 ± 0.6 | |
| | 1.5 | 976 ± 5 | 1120 ± 8 | 2.7 ± 0.5 | |

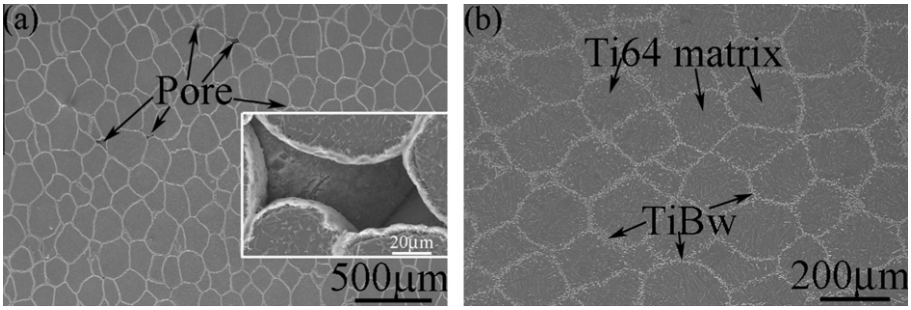


**Fig. 2.** SEM micrographs of 5 vol.%TiBw/Ti64 composites with a novel network microstructure fabricated at (a) 1000 °C and (b) 1300 °C by hot pressing reaction.

temperature further softens the local matrix. The above two factors largely decrease the resistance of hot deformation to form the compact composite. Additionally, it can be clearly seen from Fig. 2 that the width of the TiBw reinforcement network, namely TiBw length, of the composite fabricated at 1300 °C is obviously wider than that of the composite fabricated at 1000 °C. The reason is that the diffusion distance and speed of B element can be largely increased with increasing the sintering temperature.

Fig. 3 shows that the effects of sintering temperature on the microstructure of 5 vol.%TiBw/Ti64 composites with a network microstructure. Fig. 3a not only shows the large pores in the composite but also shows an premature TiBw shell and crack (as shown in the insert image) between adjacent units, which are probably harmful to the tensile properties of the composite. As seen from the pore region, the shell is ripped due to large deformation. The ripped deformation indicates that the specific surface of Ti64 matrix particle increases with increasing the relative density, which can further increase the contiguity of Ti64 matrix. The ductility of the compact composites with a quasi-continuous network microstructure mainly depended on the contiguity of Ti matrix and the size of Ti64 matrix particle. Fig. 3b shows that the *in situ* synthesized fine TiB whiskers together with their parents form a similar thorn wall due to inadequate reaction. It is quite obvious that this premature microstructure is harmful to the tensile properties of the composite. By comparing Fig. 3c and d with a and b, it is seen that the size and quantity of the pore is remarkably decreased, and the aspect ratio of TiB whiskers is remarkably increased by increasing sintering temperature to 1100 °C. In fact, the length of TiBw is remarkably increased but the diameter remains unchanged. Although a better bonding without crack between the adjacent units is formed, an obvious thorn wall still interdicts the contiguity of the neighboring Ti matrix. At 1200 °C, all of the pore, crack and thorn wall disappear and are replaced by superior bonding, coarse and strong TiB whiskers and the inter contiguity of the adjacent Ti64 matrix through the network boundary, which construct a quasi-continuous network microstructure. However, increasing the sintering temperature from 1200 °C to 1300 °C has not brought perceptible change of TiBw morphology and the microstructure of the composite. It is reasonable to predict that the optimal sintering temperature is 1200 °C and the composites fabricated at 1200 °C can exhibit an as-expected superior combination of tensile properties.

Fig. 4 shows SEM micrographs of the 5 vol.%TiBw/Ti64 composites fabricated at 1200 °C but for different holding times. It can be seen that there is rarely any difference by comparing Figs. 4a and b and 3e. This phenomenon indicates that the $TiB_2$ raw material can completely and quickly disintegrate once the sintering temperature reaches 1200 °C. That is to say, the sintering temperature is a much more important parameter than other parameters that influence the microstructure of the composites.

No matter what the sintering parameter, the prepared composites can present a network structure as shown in the Figs. 2–4. However, the quasi-continuous network microstructure of TiBw/Ti64 composites has to be achieved at sintering temperatures equal to or higher than 1200 °C. The quasi-continuous network structure can be viewed as that one continuous TiBw-rich boundary phase with a higher reinforcement volume fraction encapsulates one dispersed TiBw-lean phase with a much lower reinforcement volume fraction, in terms of Hashin–Shtrikman (H–S) theorem [10]. Therefore, the present network structure can be treated as the one with H–S upper bound structure [10] or the multi-scale hierarchical structures proposed by Lu [11]. Compared with the conventional homogeneous structure, the strengthening effect can be further enhanced by assembling components in a controlled way to form a novel reinforcement hierarchical structure [11]. In other words, the stronger network boundary phase can dominate the behaviors of the composites. Therefore, the composites with a premature network structure probably exhibit inferior mechanical properties, while the composites with the mature quasi-continuous network microstructure must exhibit a superior combination of tensile properties.

Fig. 5 shows some unique TiB whisker features formed due to the novel network distribution. Firstly, a dowel-like structure (Fig. 5a) can be easily formed due to the special B27 structure and network distribution of TiB whisker [12,13]. Secondly, TiBw can easily touch each other due to the high local volume fraction in the boundary region, the self-joining structure (Fig. 5a) can be easily formed by the siamese growth of the touching TiB whiskers with a similar crystal orientation. Thirdly, claw-like structure (Fig. 5b) of TiBw can be observed for the first time, which was

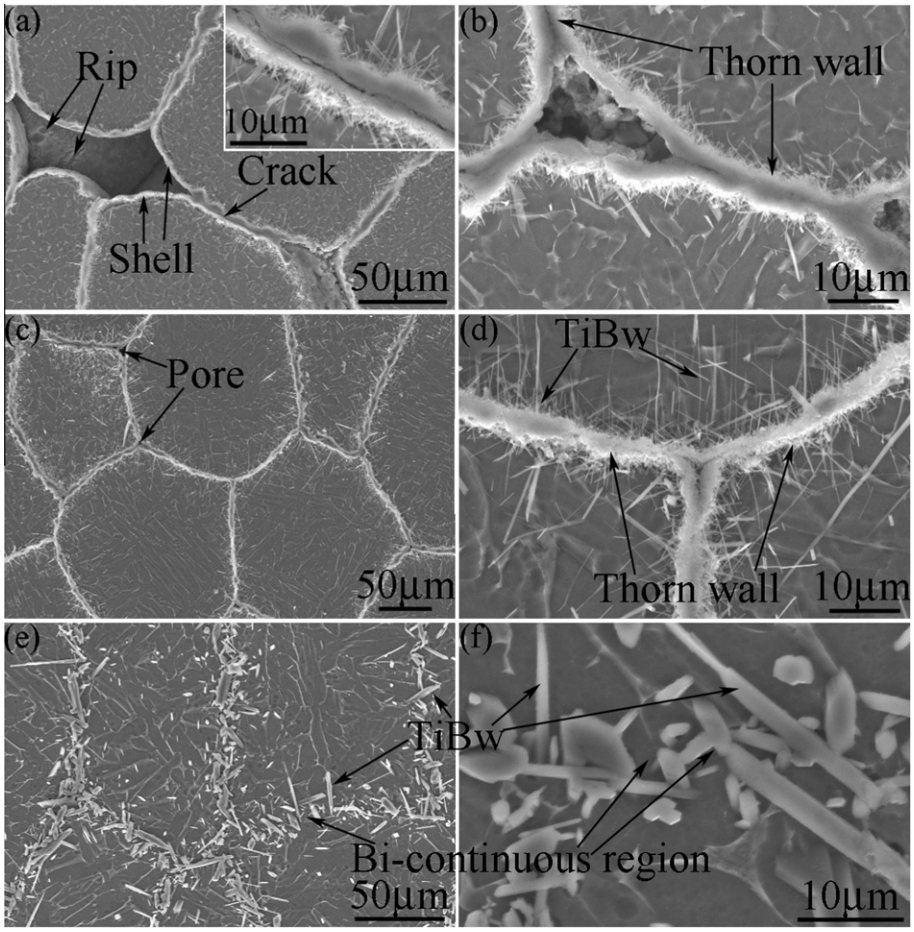


**Fig. 3.** SEM micrographs of TiBw/Ti64 composites fabricated at different temperatures: (a and b) 1000 °C, (c and d) 1100 °C, (e) 1200 °C, (f) 1300 °C; (a and c) at relatively low magnifications and (b and d) at relatively high magnifications.

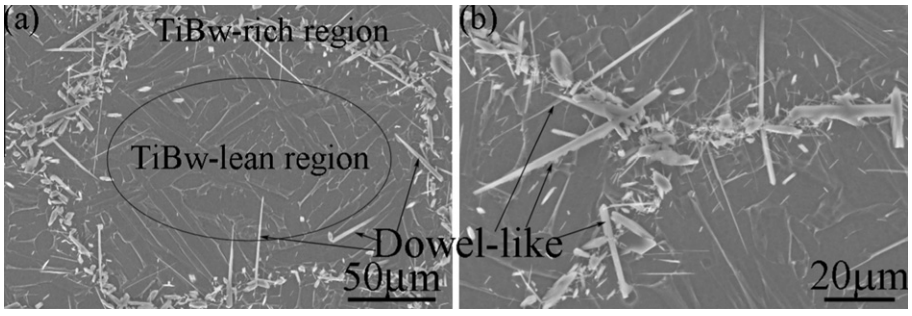


**Fig. 4.** SEM micrographs of TiBw/Ti64 composites fabricated at 1200 °C for: (a) 0.5 h and (b) 1.5 h.

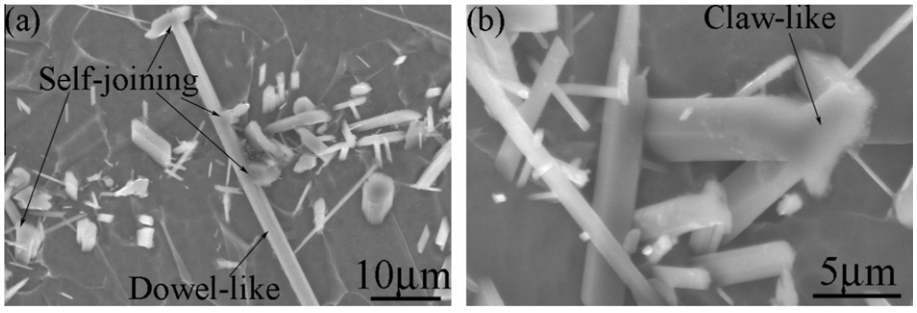


**Fig. 5.** SEM micrographs of some unique features of TiB whiskers: (a) dowel-like and self-joining structures, and (b) claw-like structure.

probably formed by nucleation and growth of different TiB whiskers from one $TiB_2$ polycrystal parent. Therefore, the unique dowel-like, self-joining and claw-like structures (Fig. 5) together with the network distribution construct one 3D whisker architecture, which can further improve the mechanical properties of TMCs [14–16]. On the one hand, the dowel-like TiB whiskers can effectively link the neighboring Ti64 matrix particles, and on the other hand, the branched TiB whiskers (self-joining and claw-like whiskers) are equivalent to increase the effective length of whiskers. On a higher hierarchical scale, the self-assemble 3D whisker framework is beneficial to transfer load.

Fig. 6 shows the schematic illustration of the growth of *in situ* TiBw with special B27 crystal structure, which is unanimous in many literatures [12,13]. The formation of whisker morphology is due to that the growth speed of TiBw along [0 1 0] direction which is marked as $V_{[010]}$ is much higher than that along [1 0 0] and [0 0 1] directions marked as $V_{[100]}$ and $V_{[001]}$, respectively. The main reason is that the bonding energy of Ti–B atoms along the longitudinal [0 1 0] direction is much higher than that along the transverse [1 0 0] and [0 0 1] directions [13]. The aspect ratio of *in situ* TiBw is mainly influenced by the combination of $V_{[010]}$, $V_{[100]}$ and $V_{[001]}$, which is determined by the diffusion distance and diffusion speed of B element along the three directions. Further more, the diffusion distance and speed are mainly controlled by the sintering temperature. Therefore, the aspect ratio and morphology of *in situ* TiB whiskers are mainly determined by sintering temperatures, which is consistent with the above microstructural observation (Fig. 3). Additionally, the size and crystal styles of $TiB_2$ raw material are also crucial factors.

Fig. 7 shows schematic illustrations of some nucleation and growth features of *in situ* TiBw at different temperatures. As shown in Fig. 7a the fine $TiB_2$ powders adhere on the surface of large Ti64 particles by the low-energy milling process, which corresponds to that the low-energy milling process did not break up the large Ti64 particles as shown in the Fig. 1 [1]. Fig. 7b shows that the spherical Ti64 particles with the smallest surface area are compressed to polyhedrons, which increases the specific surface of Ti particles and dilutes the $TiB_2$ particles density on the surface of Ti64 particles. This assumption is in accordance with the rip of the premature shell in the Fig. 3a. In the beginning of the reaction as shown in Fig. 7c–e, several TiBw are probably synthesized along different directions. For this phenomenon, one probably reason is that $TiB_2$ raw material is polycrystal and thus can simultaneously form several whiskers from different grains but the same $TiB_2$ parent; another reason is that TiBw can be synthesized from different crystal faces, just different growth speeds and priorities. As in the case of a combination of the above two reasons, it is reasonable for the formation of the thorn wall (Fig. 3b and d) similar to TiB whisker cluster [17]. Moreover, the former assumption can exactly interpret the formation of the claw-like whisker structure as shown in the Fig. 5b. As shown in Fig. 7c, definite diffusion distance of B element at the lowest temperature of 1000 °C limits the growth of *in situ* TiBw along [0 1 0] direction, which encourages other whisker growth from subordinate crystal grains or faces. This representation corresponds to the existence of abundant fine TiB whiskers on the inside of the thorn wall (Fig. 3b). Up to 1100 °C, the diffusion distance or diffusion speed of B element is highly skipped along [0 1 0] direction but slightly enhanced along [1 0 0] and [0 0 1] directions, which remarkably increases the length but the diameter of TiB whiskers remains unchanged (Fig. 3d). Hot-pressing causes residual $TiB_2$ to be further embedded in the Ti matrix, which encourages the nucleation and growth of some new TiB whiskers. Therefore, TiB whiskers with so much different sizes are observed as shown in Fig. 3d. However, increasing sintering temperature up to 1200 °C, $V_{[100]}$ and $V_{[001]}$ are remarkably waken and enhanced. Therefore, coarse TiBw can be immediately synthesized which consumes the total or most of the $TiB_2$ parents and then restricts the growth along [0 1 0] direction and the formation of other subordinate TiBw. This representation corresponds not only to a lower aspect ratio (Fig. 3e and f) of TiBw but also to the unchanged morphology of TiBw synthesized at 1200 °C (Fig. 4a and b). But one large $TiB_2$ polycrystal can simultaneously form several TiB whiskers, which forms a delicate claw-like structure of TiBw as shown in Figs. 5b and 7e. As mentioned above, the $V_{[100]}$ and $V_{[001]}$ can not be further elevated with increasing the sintering temperature from 1000 °C to 1100 °C and from 1200 °C to 1300 °C, which is consistent with the similar diameters of TiBw synthesized at 1000 °C and 1100 °C, even the identical morphologies at 1200 °C and 1300 °C. Moreover, the ratio of $V_{[010]}$ to $V_{[100]}$ or $V_{[001]}$ will be stable over 1200 °C based on the identical morphology of TiBw. Additionally, the similar aspect ratio of TiBw in the composites fabricated by melted ingot over 1700 °C [18] can further demonstrate the above conclusions. In terms of analysis and comparison [2,7,8,18], the formation of the branched structures including claw-like and self-joining structures can be attributed to the $TiB_2$ polycrystal remained by low-energy milling process and the network distribution with a high local volume fraction of TiBw reinforcement.

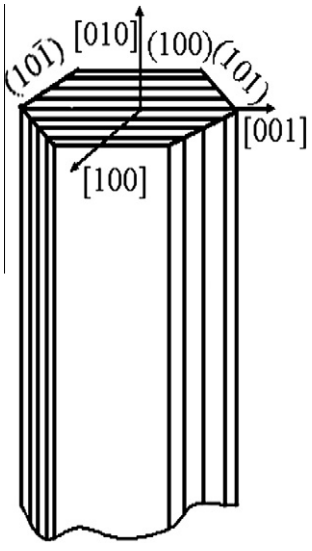


**Fig. 6.** Schematic illustration of the growth of *in situ* TiB whisker.

### 3.2. Tensile properties

Table 1 summarizes the tensile properties of the composites in order to further investigate the effect of processing parameters on mechanical properties of the 5 vol.%TiBw/Ti64 composites with a novel network microstructure. $T_{1000}t_{1.0}$ composite indicates extremely inferior tensile properties, which corresponds to the big pore and the debonding thorn wall. However, shrinking pore, increasing connection plus longer TiBw dowel-like structure can highly improve the tensile properties when the sintering temperature is elevated to 1100 °C. Further increasing sintering temperature up to 1200 °C can remarkably improve the tensile properties. The tensile properties of $T_{1300}t_{1.0}$ composite have no difference with those of $T_{1200}t_{1.0}$ composite, which is consistent with the similar morphologies of TiBw reinforcement and the network architecture. Table 1 also reveals that the holding time has hardly any influence on the tensile properties of the composites with sintering temperatures up to 1200 °C. The above similar and superior tensile properties can be attributed to the quasi-continuous network structure, strong dowel-like structure, coarse and branched TiBw

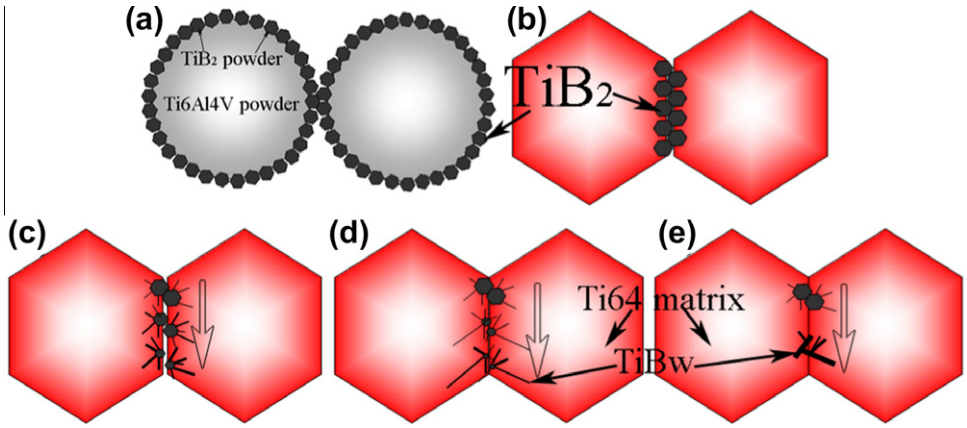


**Fig. 7.** Schematic illustrations of network distribution and the growth of *in situ* TiBw at different conditions: (a) before sintering, (b) before reaction, (c) 1000 °C, (d) 1100 °C, and (e) over 1200 °C.

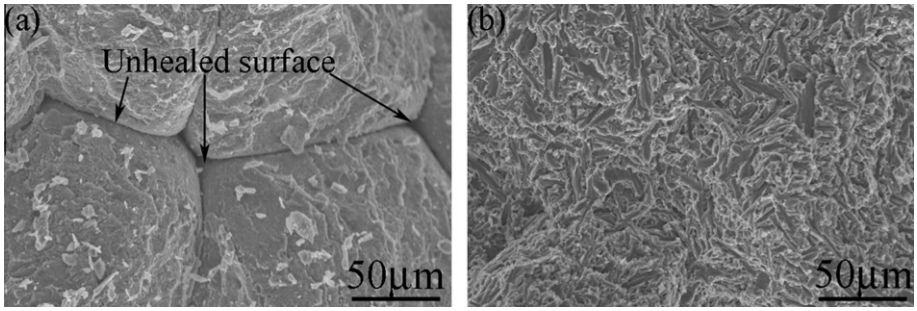


**Fig. 8.** SEM fracture surface of TiBw/Ti64 composites fabricated at (a) 1000 °C and (b) 1200 °C.

reinforcement. All the composites fabricated by one-step sintering over 1200 °C exhibit approximately 1100 MPa of tensile strength which is increased by 30% compared with that of the monolithic alloy [1], along with beyond 2.5% of elongation, which is a significant improvement compared with TMCs fabricated by the conventional PM process. It is worth pointing out that the tensile strength and ductility can be much further improved by subsequent treatment such as extrusion.

In addition, the elastic modulus of the composites increases with increasing the sintering temperatures from 1000 °C to 1200 °C, and becomes stable over 1200 °C. This can be attributed to the increasing relative density. However, as mentioned above, once the sintering temperature is above 1200 °C, the relative density and microstructure will remain stable (Figs. 3 and 4). Therefore, the composites fabricated over 1200 °C destine the identical elastic modulus and other properties. Additionally, the highest and lowest theoretical elastic modulus of quasi-isotropic 5 vol.%-TiBw/Ti64 are 123.9 GPa and 119.5 GPa, according to the H–S theorem [10]. Therefore, the elastic modulus of the present composites (123.1 GPa) is much close to the H–S upper bound. This can be attributed to the quasi-continuous network microstructure and the branched structures.

### 3.3. Fracture surface

Fig. 8 shows SEM fracture surfaces of 5 vol.%TiBw/Ti64 composites fabricated at 1000 °C and 1200 °C, respectively. Unhealed surface corresponding to the pore and crack in the Fig. 3a and b can be obviously observed in Fig. 8a. That is to say, the pore is the origin of crack, which absolutely leads to inferior mechanical properties of the composite. Additionally, TiBw can hardly found in the fracture surface due to the small size of TiBw and weak bonding by premature TiBw thorn wall structure (Fig. 3b), which determines the inferior mechanical properties of TMCs.

As shown in Fig. 8b, many whiskers were broken which indicates the superior strengthening effect of TiBw reinforcement. It is also observed that micro-voids located around TiB whiskers, which verifies the contiguity of the matrix in the TiBw-rich boundary region (Figs. 3 and 4). Moreover, it appears that matrix voids were unable to grow up and propagate due to the baffling effect of the stronger whiskers. This phenomenal is consistent with the decrease of ductility for the present composites compared with the monolithic Ti64 alloy. These features demonstrate the superior tensile properties of TiBw/Ti64 composites with a novel quasi-continuous network reinforcement distribution.

## 4. Conclusions

(1) The relative density and tensile properties of the as-sintered *in situ* TiBw/Ti64 composites is increased with increasing the sintering temperature and then remain stable thereafter.
(2) The thorn wall can be formed below 1100 °C but quasi-continuous network structure and strong TiB whiskers can be formed over 1200 °C. The quasi-continuous network microstructure of 5 vol.%TiBw/Ti64 composites can exploit superior tensile properties.
(3) The TiB whiskers with the highest aspect ratio and the coarsest whiskers can be synthesized at 1100 °C and 1200 °C due to the skips of whisker growth speed along the [0 1 0] direction and the [0 0 1] and [1 0 0] directions, respectively.

(4) The formation of dowel-like structure can be attributed to the B27 crystal structure of TiB whisker and the network distribution of $TiB_2$ raw material, while the branched TiBw structure can be formed by self-joining and multi direction growth from one $TiB_2$ polycrystal parent.

## Acknowledgement

This work is financially supported by the National Natural Science Foundation of China under Grant No. 50771039 and the Royal Society (RS)–NSFC International Joint Project under Grant No. 51011130206. Huang is supported to study at the University of Bristol for 1 year through China Scholarship Council (CSC).

## References

[1] Huang LJ, Geng L, Li AB, Yang FY, Peng HX. In situ TiBw/Ti–6Al–4V composites with novel reinforcement architecture fabricated by reaction hot pressing. Scripta Mater 2009;60:996–9.
[2] Tjong SC, Mai YW. Processing–structure–property aspects of particulate-and whisker-reinforced titanium matrix composites. Compos Sci Technol 2008;68:583–601.
[3] Huang B, Yang Y, Luo H, Yuan M. Effects of the coating system and interfacial region thickness on the thermal residual stresses in SiCf/Ti–6Al–4Vcomposits. Mater Des 2009;30:718–22.
[4] Liu D, Zhang SQ, Li A, Wang HM. Creep rupture behaviors of a laser melting deposited TiC/TA15 in situ titanium matrix composite. Mater Des 2010;31:3127–33.
[5] Ma FC, Lu WJ, Qin JN, Zhang D, Ji B. The effect of forging temperature on microstructure and mechanical properties of in situ TiC/Ti composites. Mater Des 2007;28:1339–42.
[6] Wang MM, Lu WJ, Qin JN, Ma FC, Lu JQ, Zhang D. Effect of volume fraction of reinforcement on room temperature tensile property of in situ (TiB+TiC)/Ti matrix composites. Mater Des 2006;27:494–8.
[7] Gorsse S, Miracle DB. Mechanical properties of Ti–6Al–4V/TiB composites with randomly oriented and aligned TiB reinforcements. Acta Mater 2003;51:2427–42.
[8] Morsi K, Patel VV. Processing and properties of titanium–titanium boride (TiBw) matrix composites – a review. J Mater Sci 2007;42:2037–47.
[9] Ni DR, Geng L, Zhang J, Zheng ZZ. Fabrication and tensile properties of *in situ* TiBw and TiCp hybrid-reinforced titanium matrix composites based on Ti–$B_4C$–C. Mater Sci Eng A 2008;478:291–6.
[10] Hashin Z, Shtrikman S. A variational approach to the theory of the elastic behaviour of multiphase materials. J Mech Phys Solids 1963;11:127–40.
[11] Lu K. The future of metals. Science 2010;328:319–20.
[12] Panda KB, Ravi Chandran KS. First principles determination of elastic constants and chemical bonding of titanium boride (TiB) on the basis of density functional theory. Acta Mater 2006;54:1641–57.
[13] Meng Q, Feng H, Chen G, Yu R, Jia D, Zhou Y. Defects formation of the in situ reaction synthesized TiB whiskers. J Cryst Growth 2009;311:1612–5.
[14] Rodríguez-Manzo JA, Wang MS, Banhart F, Bando Y, Golberg D. Multibranched junctions of carbon nanotubes via cobalt particles. Adv Mater 2009;21:4477–82.
[15] Tao X, Liu J, Koley G, Li X. B/$SiO_x$ nanonecklace reinforced nanocomposites by unique mechanical interlocking mechanism. Adv Mater 2008;20:4091–6.
[16] Peng HX, Fan Z, Mudher DS, Evans JRG. Microstructures and mechanical properties of engineered short fibre reinforced aluminium matrix composites. Mater Sci Eng A 2002;335:207–16.
[17] Ni DR, Geng L, Zhang J, Zheng ZZ. Effect of $B_4C$ particle size on microstructure of *in situ* titanium matrix composites prepared by reactive processing of Ti–$B_4C$ system. Scripta Mater 2006;55:429–32.
[18] Sen I, Tamirisakandala S, Miracle DB, Ramamurty U. Microstructural effects on the mechanical behavior of B–modified Ti–6Al–4V alloys. Acta Mater 2007;55:4983–93.